IEEE Access
Multidisciplinary | Rapid Review | Open Access Journal

Received January 7, 2020, accepted February 17, 2020, date of publication February 21, 2020, date of current version March 3, 2020.

Digital Object Identifier 10.1109/ACCESS.2020.2975674

Dynamic Economic Dispatch With Maximal Renewable Penetration Under Renewable Obligation

THABO G. HLALELE[1], RAJ M. NAIDOO[1], (Senior Member, IEEE), JIANGFENG ZHANG[2], AND RAMESH C. BANSAL[3], (Senior Member, IEEE)

[1]Department of Electrical, Electronic and Computer Engineering, University of Pretoria, Pretoria 0002, South Africa
[2]Department of Automotive Engineering, Clemson University at Greenville, Greenville, SC 29607, USA
[3]Department of Electrical Engineering, University of Sharjah, Sharjah, United Arab Emirates

Corresponding author: Thabo G. Hlalele (greg.hlalele@gmail.com)

This work was supported in part by the South African National Development Institute and in part by the University of Pretoria.

ABSTRACT This paper presents a multi-objective dynamic economic dispatch model with renewable obligation requirements. The two objective functions that are presented in this paper aim to increase the level of renewable energy sources in the grid while minimising the total operating cost and respecting the spinning reserves required to maintain continuity of supply. The proposed model incorporates thermal power plants, photovoltaic and wind power plants into the grid. The paper presents a Pareto optimal solution which is a compromise between maximising the renewable energy source generation while minimising the operating costs. A renewable obligation policy is implemented in the proposed model to ensure that renewable energy source generators are utilised and any failure to attain the required renewable obligation is penalised in line with the renewable obligation framework. The proposed model is modified into a single objective optimisation problem and numerical tests are performed on the modified IEEE 24 RTS system and IEEE 118 bus system to test the effectiveness of the model. A comparative study evaluates the impact of the proposed model on the traditional dynamic economic dispatch in terms of the achieved renewable energy source penetration level and economic performance. The numerical simulations show that the proposed model is robust and can attain high renewable energy source penetration levels.

INDEX TERMS Dynamic economic dispatch, multi-objective optimisation, Pareto optimal solution, photovoltaic power plants, renewable energy obligation, renewable energy sources, spinning reserve requirement, Weibull probability density function, wind farms.

NOMENCLATURE

INDICES AND SETS:

b	Index of buses.
g	Index of thermal generators.
i	Index of all equality constraints.
j	Index of all inequality constraints.
k	Index of all objective functions.
v	Index of photovoltaic generators.
m	Index of wind generators.
l	Index of transmission lines.
t	Index of time period.
r	Index of generator spinning reserves.
T	Time interval period.
N_I	Set of all equality constraints.
N_J	Set of all inequality constraints.
N_G	Set of thermal generators.
K	Set of all objective functions.
N_M	Set of wind generators.
N_V	Set of photovoltaic generators.
N_R	Set of generator spinning reserves.
N_S	Set of battery energy storage systems.
N_L	Set of transmission lines.
N_B	Set of buses.

The associate editor coordinating the review of this manuscript and approving it for publication was B. Chitti Babu.

PARAMETERS:

C_g	Thermal generator g marginal cost.
C_m	Wind generator m tariff cost.
C_v	PV generator v tariff cost.
C_r	Thermal generator spinning reserve r operating cost.
γ	Renewable energy penalty cost in US dollars.
α	Renewable energy obligation requirement.
ρ	Spinning reserve cost coefficient of the gth thermal generator in $\$/MWh$.
ζ	Wind generator cost in $\$/MWh$.
φ	PV generator cost in $\$/MWh$.
π	Wind speed in m/s.
Ω	Solar irradiance in W/m^2.
Ω_{std}	Solar irradiance in the standard environment.
σ	Weibull distribution scale parameter in m/s.
β	Weibull distribution form parameter.
R_c	A certain radiation point.
$f_\Omega(\Omega)$	Solar irradiance probability distribution function.
$f_\pi(\pi)$	Wind speed probability distribution function.
$f_m(P_m)$	Probability distribution of random variable P_m.
$f_v(P_v)$	Probability distribution of random variable P_v.
$P_{b,t}$	System demand at bus b and time t.
$P_{g,min}$	Minimum output power from the gth thermal generator in MW.
$P_{g,max}$	Maximum output power from the gth thermal generator in MW.
$P_{l,t}$	Transmission line power flow at time t.
$P_{m,t,gen}$	Generated output power from the mth wind farm at time t.
$P_{v,t,gen}$	Generated output power from the vth PV plant at time t.
$SRR_{r,max}$	Maximum spinning reserve requirement for the gth thermal generator in MW.
$SSRR$	System spinning reserve requirement for operating all thermal generators in MW.
UR_g, DR_g	Ramp up and down limit for the gth thermal generator in MW/h.

DECISION VARIABLES:

$P_{g,t}$	Scheduled output power for thermal generator g at time t
$P_{r,t}$	Scheduled output power for thermal generator spinning reserve r at time t
$P_{m,t}$	Scheduled output power for wind farm m at time t
$P_{v,t}$	Scheduled output power for PV generator v at time t.

I. INTRODUCTION

In the past decade there has been an acceleration in the integration of variable renewable energy sources (RES) in the power grid as part of the transition towards decarbonisation of the electricity sector. The decarbonisation was motivated by the need to reduce greenhouse gas emission caused by thermal generators which threatens global climate change. Although greenhouse gas emission can be attributed to many other sectors such as residential, transport, industrial, and commercial, the largest contribution comes from the industrial sector, from electricity generation [1]. The EU has set a binding target for all its member states to reduce greenhouse gas emissions by 20% by 2020, whilst in South Africa a target has been set to reduce the total energy supply from conventional thermal generators to less than 30% by 2030 and a further 10% by 2050 [2].

There are generally two policy frameworks used to encourage the penetration of RES for a complete energy mix. The two frameworks are divided into quantity based and tariff-based instruments. Tariff and quantity-based instruments are the key funding frameworks used by regulators to encourage investment in renewable energy. A tariff-based instrument, such as the Feed-in Tariff (FIT), provides an economic incentive for generating electricity using RES. This type of instrument guarantees grid access, long term contracts for the electricity producer and purchase prices that are based on RES generation costs [3], [4]. In contrast, a quantity-based instrument is utilised to keep role-players within the energy value chain accountable for meeting the minimum renewable energy targets. A renewable obligation (RO) is a quantity-based tariff instrument that requires electricity suppliers to adhere to the minimum renewable energy production quota. The failure to meet the obligation quota is penalised, and this approach encourages the generation companies to comply with their RES obligation. The renewable obligation certificates (ROC) are also awarded to companies that comply with their RES obligation which can further be traded in the market and typically one ROC certificate is equivalent to 1 MWh of renewable energy production. This quota mechanism has been adopted by countries such as Great Britain, Italy, Chile, Belgium and other parts of the US [5], [6].

A generation expansion planning (GEP) model is presented in [5], where the approach is to design an effective and efficient incentive policy that increases the level of RES injection in the grid. The approach adopted in [5], focuses on the inception level instead of the operational level. The design approach concept is based on stimulating an investment policy that increases the level of RES injection by specifically focusing on improving the cost competitiveness of RES in the short term by using a bi-level optimisation approach. The bi-level optimisation finds a minimum trade-off between economic benefit and environmental impact and the most efficient incentive policy that can achieve maximum RES penetration. In [6], a GEP problem is presented that evaluates different RES incentive schemes such as quantity based and tariff-based instruments. The work presented in [6] shows the impact of RES incentives and CO_2 mitigation policies in the GEP framework from the generation companies' point of view. The inclusion of RES in the grid has mostly been considered from the GEP perspective, with less focus on the operation point of view. A review of the different RES supporting schemes is presented in [7], for increasing the RES

level in the grid; and the impact of feed-in tariff is analysed from the priority dispatch rule, negative prices and economic compensation.

In [8], a dynamic FIT is introduced for a wind farm that is integrated with thermal generators to encourage the maximum export of wind power generation without adversely affecting the conventional generators. The concept of dynamic cost coefficient is introduced in order to account for the variable wind speed and fluctuating power demand which increases the wind penetration in the overall energy mix. The economic dispatch model is presented to account for the hourly dispatch of thermal and wind generators using fuzzy logic to provide the best dynamic cost coefficient of the wind generators. In [9], a unit commitment model is used to quantify the operational impacts of incentivising RES generation when the energy prices are negative. The negative prices affect the flexibility of system operation and increase the thermal generator cycling costs. Therefore, it is important to consider the increase in RES penetration from an operational point of view such as economic dispatch within the renewable energy obligation framework. Fundamentally, the classical economic dispatch problem optimises the schedule power of each generator in order to minimise the fuel costs while meeting the demand and machine ramp rates [10], [11].

The impact of increasing the RES in the network has resulted in a high requirement for spinning reserves which is used to balance the deviations emanating from variable RES generation. This increased level of RES penetration has resulted in a high cycling rate for thermal generators and has subsequently increased the maintenance costs of thermal generators and the overall operating expenses. Reference [12] presents, a security constrained economic dispatch (SCED) which focuses on the level of uncertainty caused by the increased level of RES penetration while considering the operational reserves. The approach proposed in [12] studies the impact of wind reserve margins from the market implication perspective by considering reserves policies that can mitigate the uncertainty associated with wind power generation. A probabilistic spinning reserve approach is presented in [13], which increases the integration of wind power generation using an algorithm that integrates the stochastic wind forecast of a day ahead security constrained unit commitment approach. In [14], a two stage SCED with robust optimisation is presented for reserve requirement and energy scheduling model where the operational risk is presented using a Wasserstein ball-based method. The model presented minimises the projected operating costs of producing energy while providing spinning reserves and satisfying the operational constraints.

A classical economic dispatch that incorporates the wind energy and system spinning reserves for optimal energy scheduling is presented in [15]. The model includes the under and over estimation of the available wind energy in the optimal scheduling of different generators. A similar approach is presented in [16] and [17] where a day ahead model is presented in a SCED model that minimises the spinning reserve requirements and ancillary services for high RES penetration in a FIT environment. The importance of spinning reserve requirements is further illustrated in [18], where a hybrid method is used for allocating SR in a risk based deregulated electricity market for the operation of a reliable system which includes high wind penetration. A new approach is presented in [19], where energy storage system (ESS) is used to complement high level of wind penetration in order to minimise transmission infrastructure expansion and increase the RES penetration in a FIT environment. The energy storage improves the accommodation of renewable generation by mitigating the emergency overflow under the post contingency state. In [20], a stochastic security constrained unit commitment with wind energy considering coordinated operation of price-based demand response and energy storage is presented. The price-based demand response is formulated as a price response dynamic demand bidding mechanism. A multi-objective stochastic economic dispatch is presented in [21], which is based on two objective functions. One objective function minimises the expected power purchase costs and the second objective function minimises the pollution of gas emission from conventional thermal generators. A Pareto based algorithm is used to solve the multi-objective optimisation problem using the normal boundary intersection method. Moreover, the stochastic dispatch method is approached from scenario-based decomposition.

None of the referenced studies have investigated the RES penetration from an obligation point of view. Instead, they have focused on the underestimation and over-estimation of RES on the cost function to compensate for under performance and over performance of the RES [22] - [24]. In this study, a novel multi-objective function that includes the RES quota is presented in order to minimise the operating costs of thermal generators, spinning reserve, and maximise the RES penetration. The basis for this approach emanates from the need to achieve a moderate energy mix in the network that includes RES and thermal generators. The model sets a target obligation that the SO imposes on the network. If the generators do not achieve a minimum obligation set out, then a penalty is imposed to the thermal generators. Moreover, it is important to note that in most practical systems, the RES contributes all its generated energy into the grid if it does not exceed the contractually agreed achieved capacity. This means there is no need for penalising the RES for over supply since a curtailment is already implemented in the operation of the RES generators. Hence, the only penalty that is imposed is the failure to meet the minimum quota set out by the SO. The contributions of this work are listed below:

1) A RO policy framework is mathematically modelled and incorporated into a SCED to allow maximum RES penetration while penalizing generation companies for not complying with the minimum RES quota. This model is aligned to the quantity-based instrument which measures the quantity of RES injected into the grid to achieve a cost-effective energy mix.

2) A multi-objective optimisation model is presented with two objective functions. The first objective function is related to the minimisation of the total operating cost and spinning reserve cost of the thermal generators. The RO model is included in the first objective function to ensure a minimum RES quota is achieved and if it is not achieved a penalty is imposed to thermal generators. The second objective function maximises the total RES energy generated from wind and photovoltaic (PV) power plants.

The contents of this paper are organised into six sections. In Section II the dynamic economic dispatch (DED) model is developed to include thermal and RES generators and the RO model. In Section III, a probability density function (PDF) for the wind speed and solar irradiance using the Weibull function is developed. In Section IV, the feasibility and efficiency of the proposed method are investigated on two test systems. In Section V, the results from the two test systems are discussed in detail and finally in Section VI, the conclusions are drawn.

II. PROBLEM FORMULATION

The approach considered in this paper assumes that wind and PV power generators are non-dispatchable. The following assumptions are made for the formulation of the DED problem with RES obligation;

1) All the RES (wind and PV) must be consumed first and the thermal generators must reduce their generation capacity to give preference to RES generators.
2) An hourly dispatch period is considered in all the case studies.
3) All RES are non-dispatchable and cannot be used as part of spinning reserves unless they have storage.
4) The SO is responsible for dispatching all the generators including RES generators.
5) Only thermal generators can be used for spinning reserve.
6) All the RES generators are owned by independent power producers (IPP).
7) We simplify the RO model by ignoring the secondary trading market of ROC.

A. OBJECTIVE FUNCTION

The objective function is made up of two objective functions, i.e. the fuel cost minimisation with renewable energy obligation requirement, and the RES energy maximisation function. The objective functions are as follows:

$$\min J_1 = C_T \tag{1}$$

$$\max J_2 = E_{RES} \tag{2}$$

1) MINIMISATION OF THE TOTAL OPERATING COST C_T

The operating cost in (3), is made up of two parts. The first part of (3), is related to the operating cost for all generators. It includes the fuel cost for operating thermal generators, the spinning reserve cost to guarantee continuity of supply and the energy cost incurred by the SO to pay the IPPs for the RES generators. The second part of (3), is related to the policy requirement from the quantity-based instrument which is known as RO [25]–[27]. This ensures that a total quantity of energy exported to customers includes a certain percentage of RES generation per day. The level of obligation is normally provided on an annual basis to the electricity suppliers and all the renewable energy suppliers provide their generated capacity on a monthly basis. The conventional electricity suppliers or generation companies are responsible for ensuring that a portion of their electricity supply comes from RES generators. If the generation companies do not meet their renewable obligation, a penalty is imposed. In the second expression of (3), Υ represents the RO cost which is further calculated in (8).

$$C_T = \sum_{t=1}^{T} \left(\sum_{g=1}^{N_G} C_g(P_{g,t}) + \sum_{r=1}^{N_R} C_r(P_{r,t}) + \sum_{m=1}^{N_M} C_m(P_{m,t}) + \sum_{v=1}^{N_V} C_v(P_{v,t}) \right) + \Upsilon \tag{3}$$

$C_g(P_{g,t})$ is the generator cost function which is a quadratic equation as shown in (4), where the units for the cost coefficients are $\$/MWh^2$, $\$/MWh$, and $\$/h$ and the generator spinning reserve cost is a linear function as shown in (5). In this paper, the wind and PV plants are owned by the IPPs, therefore the SO must pay a price proportional to their scheduled power. The cost function for RES is given in (6) and (7).

$$C_g\left(P_{g,t}\right) = \sum_{g=1}^{N_G} \left(a_g P_{g,t}^2 + b_g P_{g,t} + c_g \right) \tag{4}$$

$$C_r\left(P_{r,t}\right) = \rho_r P_{r,t} \Delta t \tag{5}$$

$$C_m\left(P_{m,t}\right) = \zeta_m P_{m,t} \Delta t. \tag{6}$$

$$C_v\left(P_{v,t}\right) = \varphi_v P_{v,t} \Delta t. \tag{7}$$

The RO mathematical model is shown in (8).

$$\Upsilon = \gamma \left(\alpha \sum_{t=1}^{T} \left(\sum_{g=1}^{N_G} P_{g,t} + \sum_{m=1}^{N_M} P_{m,t} + \sum_{v=1}^{N_V} P_{v,t} \right) - \sum_{t=1}^{T} \left(\sum_{m=1}^{N_M} P_{m,t} + \sum_{v=1}^{N_W} P_{v,t} \right) \right)^{+} \tag{8}$$

The α value in (8), is the required RO which means that a portion of the total scheduled output power must come from RES, or else a penalty cost is imposed for the undelivered renewable generation. The notation $\Upsilon(\cdot)^+$ is the sigmoid function which is equal to γ if the RES obligation is unattained and 0 otherwise. The γ value in (8), is the penalty value that must be paid by generation companies if they do not meet the annual RES obligation. In this paper, the obligation is set daily [28]–[30] and the thermal generation companies

are required to produce a percentage of their energy from RES. The generation companies' can also buy ROC from the eligible renewable electricity companies to complement their RES energy production shortfall. These ROCs are presented to the independent regulator to demonstrate compliance to the RO. If the thermal generation companies do not have enough ROC or renewable energy production to meet their obligation, then a penalty is paid to the SO.

2) MAXIMISATION OF THE RENEWABLE ENERGY PENETRATION

The second objective function aims to maximise the injection of renewable energy into the grid. It is worth noting that the second objective on the maximum renewable energy is not completely covered by the minimisation of RO penalty cost in the first objective function. This is because although the renewable energy obligation can be achieved in the first objective function the amount of renewable energy scheduled to the grid may not be maximal. With the second objective function, the amount of dispatched renewable energy must be maximised to overcome the limitation of merely meeting the obligation without maximising the RES energy penetration. The second objective function is shown in (9).

$$E_{RES} = \sum_{t=1}^{T} \left(\sum_{m=1}^{N_M} P_{m,i,t} \Delta t + \sum_{v=1}^{N_V} P_{v,t} \Delta t \right) \tag{9}$$

B. CONSTRAINTS

The DED problem under investigation has five constraints which are considered as hard or soft constraints. These constraints are:

1) Real power balance which represents the sum of all generating units i.e. the thermal generators, wind power generators and PV plant generators that should meet the forecast demand as given in (10).

$$\sum_{g=1}^{N_G} P_{g,t} + \sum_{m=1}^{N_M} P_{m,t} + \sum_{v=1}^{N_V} P_{v,t} = \sum_{b=1}^{N_B} P_{b,t} \quad \forall t \tag{10}$$

2) Generator ramp rate limits: This is only applicable to thermal generators. The ramp up (UR) and ramp down (DR) units are in MW/h as given in (11).

$$P_{g,t} - P_{g,t-1} \leq UR_g \quad \forall t \tag{11a}$$
$$P_{g,t-1} - P_{g,t} \leq DR_g \quad \forall t \tag{11b}$$

3) Generator limits: The generator limits are applicable to both thermal generators and RES generators. Equations (12) to (13) show the thermal generator limits. Since $P_{m,r}$ and $P_{v,r}$ are the dispatched wind and solar power into the power system, they are represented by (14) and (15), where the top limit is the forecast wind power generation and solar power generation at time t respectively, which include both the amount of power dispatched to the network and the remaining amount which is either consumed locally or curtailed due to line capacity limit.

$$\bar{P}_{g,t} \leq min(P_{g,max}, P_{g,t-1} + UR_g) \quad \forall t \tag{12}$$
$$\underline{P}_{g,t} \geq max(P_{g,min}, P_{g,t-1} - DR_g) \quad \forall t \tag{13}$$
$$P_{m,t} \leq P_{m,t,gen} \quad \forall t \tag{14}$$
$$P_{v,t} \leq P_{v,t,gen} \quad \forall t \tag{15}$$

4) Spinning reserve constraints:

$$P_{g,t} + P_{r,t} \leq P_{g,max} \quad \forall g, t \tag{16}$$
$$0 \leq P_{r,t} \leq SRR_{r,max} \quad \forall g, t \tag{17}$$
$$\sum_{r=1}^{N_R} P_{r,t} \geq SSRR \quad \forall t \tag{18}$$
$$\sum_{g=1}^{N_G} P_{g,t} + \sum_{r=1}^{N_R} P_{r,t} \geq \sum_{b=1}^{N_B} P_{b,t} \quad \forall t \tag{19}$$

where $P_{r,t}$ is the reserve contribution of unit g during time interval t. Constraint (16), shows that the sum of the thermal generator and spinning reserves is limited by the maximum thermal generator limit. Constraint (17), represents the maximum reserve contribution for each generator where $SRR_{r,max}$ is the maximum contribution of unit g to the reserve capacity. Constraint (18), requires that the total system spinning reserves be provided during period t and (19), simply means that the total generation and spinning reserve must be able to support the demand without the use of RES generators.

5) Network transmission constraints: For the economic dispatch problem, only the active power of the transmission line under RES forecast is considered, as shown in (20).

$$-P_{l,max} \leq P_{l,t} \leq P_{l,max} \; \forall l, t \tag{20}$$

The transmission line power of line l at time interval t, which is calculated by DC power flow and disregards system losses for large size power systems as shown in (21), [31] and [32]. A SCED approach is used in order to ensure that the power delivered matches the demand while ensuring that the transmission limits are respected.

$$P_{l,t} = \sum_{g=1}^{N_G} G_{l,g} P_{g,t} + \sum_{m=1}^{N_M} F_{l,m} P_{m,t} + \sum_{v=1}^{N_V} H_{l,v} P_{v,t} - \sum_{b=1}^{N_B} D_{l,b} P_{b,t} \tag{21}$$

where $G_{l,g}$, $F_{l,m}$, $H_{l,v}$ and $D_{l,b}$ denote the active power transfer coefficient factor between line l and thermal generator, wind farms, solar plant and loads; $P_{b,t}$ is the demand at bus b at time t.

In summary, the optimisation problem is formulated incorporating two objective functions; (1) and (2), which are subject to constraints, (10) - (21).

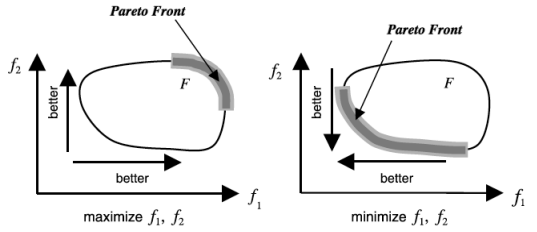

FIGURE 1. Pareto fronts for a bi-objective optimisation problem [35].

C. FORMULATION OF MULTI-OBJECTIVE OPTIMISATION MODEL

The proposed multi-objective optimisation model presented in the previous section is presented in its compact form as follows:

$$\min J(x) = \{J_1(x), J_2(x), \cdots, J_k(x)\} \quad \forall k \in K \tag{22}$$

$$\text{s.t } h_i(x) = 0; \quad \forall i \in N_I \tag{23}$$

$$g_j(x) \leq 0; \quad \forall j \in N_J \tag{24}$$

where $J_1(x)$ to $J_k(x)$ represent multiple objective functions in (1) and (2) where the value of K is 2 and x is the output vector which consists of an optimal dispatch solution for thermal and RES generators. The equality constraint in (10) is indicated by (23) and the inequality constraints from (11) to (21) are denoted by (24).

1) PARETO OPTIMAL SOLUTION

The multi-objective optimisation problem in (22) to (24), can be solved using the Pareto optimality principle. The optimal solution x^* in the feasible design space S is the Pareto optimal solution if and only if there exists no other point x in the set S such that $J(x) \leq J(x^*)$ with at least one $J_k(x) < J_k(x^*)$. The set of all Pareto optimal points refers to an optimal solution that is a compromise between the two objective functions. It also follows that an efficient solution exists if a point x^* in the feasible design space S is efficient and there is no other point in x in the set S such that $J(x) \leq J(x^*)$ with at least one $J_k(x) < J_k(x^*)$. Otherwise, x^* is inefficient. Therefore, the set of all efficient points is called the efficient frontier. The Pareto optimal set is on the boundary of the feasible criterion space which also has a unique point called the Utopia point. A point J^0 in the criterion space is called the utopia point if $J_k^0 = min\{J_k(x)\}$ for all x in the set S [33], [34]. This point is obtained by minimising each objective function without consideration of the other objective functions. Fig. 1, shows the Pareto fronts for bi-objective minimisation and maximisation problems.

It also shows that the direction of the Pareto front depends on whether the bi-objective function is maximisation or minimisation as illustrated by objective functions f_1 and f_2. The Pareto optimal solutions show that there is no single dominant solution in the Pareto frontier and thus there is a set of solutions that can gives an optimal Pareto solution. Moreover, it is clear from the Pareto frontier that there is a trade-off associated with each Pareto point.

2) NORMALISING OBJECTIVE FUNCTIONS

Since there are two objective functions that have different meanings and order of magnitudes, it is important to normalise the objective functions in order to reduce the difficulty in comparison. It is usually necessary to transform the objective functions so that they all have similar orders of magnitude. The objective functions are normalised in (25), as follows:

$$J_k^{norm} = \frac{J_k(x) - J_k^0}{J_k^{max} - J_k^0}, \ \forall k \in K \tag{25}$$

where J_k^0 is the best point also known as the Utopia point of the objective functions and J_k^{max} is the worst point of the objective functions. The overall objective function J_k^{norm} will give values within the range of 0 and 1.

3) WEIGHTED SUM OBJECTIVE FUNCTION

The Pareto frontier is generated using the weighted sum approach where each point of the weighted sum gives a Pareto point. This is achieved by uniformly changing the weights from 0 to 1, which provides a series of Pareto points on the Pareto frontier. The two objective functions in (1) and (2) are presented in (26).

$$J^{norm}(x) = \lambda_1 J_1^{norm}(x) - \lambda_2 J_2^{norm}(x) \tag{26}$$

The weights are varied between 0 and 1 such that their sum is equal to 1. In order to generate the equidistant points for the weights on the Utopia line, the weight is selected as follows in (27) and (28):

$$\lambda_1 = q/w = 0, 0.02, 0.04, \cdots, 1. \tag{27}$$

$$\lambda_2 = 1 - q/w = 1, 0.98, 0.96, \cdots, 0. \tag{28}$$

where q and w are the anchor points of the two single objective optimisation functions. In this paper, the q value is set as 1 and the w value is set as 50, which means there are 50 Pareto points that form the Pareto frontier. Therefore, a total of 51 equidistant Utopia points are created from the q and w.

III. MODELLING OF RENEWABLE ENERGY SOURCES

In this section the statistical modeling of Wind and PV generators is presented using the Weibull PDF.

A. WIND ENERGY SYSTEM

The intermittent output power of a wind turbine can be characterised as a random variable which is related to the wind speed at the hub of the turbine. The actual intermittent power can be represented as a function of wind speed (29), [36]. Moreover, the wind output power can be transformed from wind speed using a statistical transformation given in [37], [38].

$$P_{m,t,gen}(v_{m,t}) = \begin{cases} 0 & \text{if } \pi_{m,t} < \pi_m, \pi_{m,t} > \pi_o, \\ P_{m,r}\Gamma(t) & \text{if } \pi_m \leq \pi_{m,t} \leq \pi_r, \\ P_{m,r} & \text{if } \pi_r \leq \pi_{m,t} \leq \pi_o. \end{cases} \tag{29}$$

The wind speed $\pi_{m,t}$ is a random variable that varies over time; where π_m, π_r and π_o, are the wind turbine cut in speed, rated speed and cut out speed all in m/s. This means that the corresponding wind power is also a random variable and $\Gamma(t)$ is shown in (30).

$$\Gamma(t) = \left(\frac{\pi_{m,t} - \pi_m}{\pi_r - \pi_m}\right) \tag{30}$$

1) WEIBULL DISTRIBUTION FUNCTION

The Weibull distribution function has been used by many authors [23], [39], to model the percentage of time that the wind spends at a given speed on an annual basis. The Weibull distribution function is characterised by two parameters, namely the shape parameter κ and the scaling velocity σ as shown in (31).

$$f_\pi(\pi) = (\frac{\kappa}{\sigma})(\frac{\pi}{\sigma})^{\kappa-1} e^{(-1(\pi/\sigma)^\kappa)} \tag{31}$$

The cumulative distribution function (CDF) of the wind speed is given in (32).

$$F_\pi(\pi) = 1 - exp\left[-\frac{\pi^\kappa}{\sigma}\right] \tag{32}$$

The PDF of the wind power is random variable, $P_{m,t}$ in the m-th period when the wind speed is between cut-in and rated wind speed is given in (29). The Weibull PDF for the wind speed is transformed to the corresponding wind power distribution using the linear transformation [40]. More details can be found in [38], for the derivation of the wind power PDF. It follows from (32), that the CDF of the wind power is similar as shown in (33).

$$F_m(P_{m,t}) = \begin{cases} 0 & \text{if } P_{m,t} < 0, \\ 1 - e^{-(\frac{1+\frac{\delta p}{P_{m,r}}\pi_m}{e})^\kappa} & \text{if } 0 \le P_{m,t} \le P_{m,r}, \\ 1 & \text{if } P_{m,t} \ge P_{m,r}. \end{cases} \tag{33}$$

Therefore, the maximum forecast wind power is calculated using (34).

$$P_{m,t,gen} = P_m(\pi_{m,t}) F_{\pi,m}(P_{m,t}(\pi_{m,t})) \tag{34}$$

B. SOLAR ENERGY SYSTEM

For a PV energy system, a relationship among radiation resource, temperature and output power can be found in [23], [24], [41], which is also given by the function (35);

$$P_v(\Omega) = \begin{cases} P_{vr}(\Omega_t^2 / \Omega_{std} R_c) & \text{if } 0 < \Omega_t < R_c, \\ P_{vr}(\Omega_t / G_{std}) & \text{if } \Omega_t > Rc, \\ 0 & \text{if } G_t = 0. \end{cases} \tag{35}$$

where PV cell temperature is neglected and the solar active power generation can either be controlled by maximum power point tracking (MPPT) algorithm or be charged into batteries. This means that the maximum penetration of the PV generator is limited by the available maximum active power generation which is subject to solar irradiation and temperature [42], [43].

1) BIMODAL WEIBULL DISTRIBUTION FUNCTION

The output power of a PV plant depends on irradiance and temperature. The distribution of irradiance at a particular location usually follows a bi-modal distribution function. The distribution function is a linear combination of two unimodal functions. These unimodal functions can be modelled by Weibull, Log-normal and Beta PDF [39], [44]. In this paper a Weibull distribution as given in (36) is considered.

$$\begin{aligned} f_\Omega(\Omega_t) = {} & \beta(\kappa_1/e_1)(\Omega_t/\sigma_1)^{\kappa_1-1} e^{((-\Omega_t/\sigma_1)^{\kappa_1})} \\ & +(1-\beta)(\kappa_2/\sigma_2)(\Omega_t/\sigma_2)^{\kappa_2-1} e^{((-\Omega_t/\sigma_2)^{\kappa_2})} \end{aligned} \tag{36}$$

The Weibull PDF of solar PV output random variable is given in [39]. The maximum forecasted PV power is calculated by (37).

$$P_{v,t,gen} = P_v(\Omega_{v,t}) F_{\Omega,v}(P_{v,t}(\Omega_{v,t})). \tag{37}$$

IV. CASE STUDIES

In this section, two case studies are proposed for demonstrating the effectiveness of the proposed model. The proposed model is demonstrated on a modified IEEE Reliability Test System and IEEE 118 bus system [13], [45]. In the first test system, there are 32 thermal generators and 38 transmission lines, and all the hydro units have been replaced with thermal generators. The ramp rates and quadratic cost coefficients are taken from [13]. Four RES generators are added to buses 3, 5, 17, and 19 respectively, that is, two wind farms and two PV plants. The data for the four RES generators can be obtained from [46], [47]. The second test system consists of 54 thermal generators and 186 transmission lines. Ten additional RES generators are added onto the system at buses 1, 33, 38, 52, 68, 75, 96, 102, and 117. In the second test system, a combination of five wind farms and five PV plants is used. The details of the quadratic cost coefficients, transmission limits and generator ramp rates can be found in [45]. Moreover, the fixed demand at each bus is a portion of the total capacity at each sampling period. In this paper, the transmission flow limit is simulated by using DC power flow. A sampling interval of one hour is considered for generation dispatch and the optimisation problem is solved over a 24-hour period. In cases where RES penetration level is unattained, a penalty of \$100, 000 per day is imposed on generation companies by the SO. In all case studies, a 10% RES penetration level is used as a base scenario for comparison. In addition, the system spinning reserve requirement is based on 10% of the maximum thermal generator capacity and the spinning reserve requirement of each generator is equivalent to the maximum generator capacity. The wind turbine characteristics in terms of the cut-in speed, rated speed and cut-off speed is 3 m/s, 13 m/s, and 25 m/s respectively. The optimisation problem presented in Section II is a quadratic programming problem; the model has been implemented using MATPOWER for power system analysis [48] in order to find the power transfer distribution factors used in the DC power flow; and the MATLAB FMINCON optimisation algorithm is used as a solver on a notebook with an Intel Core i5 at 2.70 GHz and 8 GB RAM.

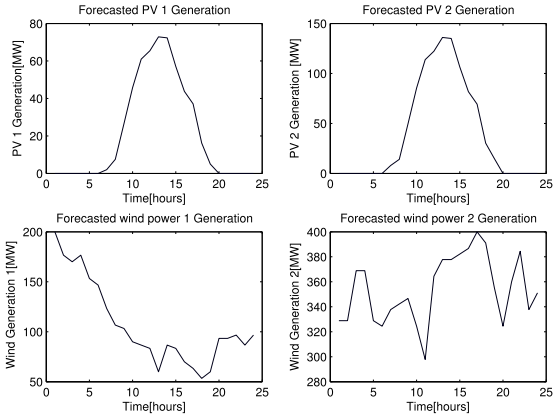

FIGURE 2. Forecasted load demand and RES generation.

The optimisation problem is solved in approximately 5 to 10 minutes depending on the number of buses involved. The IEEE 24 RTS bus system is used to demonstrate the effectiveness of the modelling considering the following cases:

1) A comparison of the traditional DED model with the proposed model in terms of the maximum RES penetration that can be achieved, the operating cost, and the spinning reserve requirements;
2) A Pareto frontier optimal solution for the multi-objective optimisation problem; and
3) The impact of RO requirement on the model sensitivity.

Thereafter, IEEE 118 test system is also used to test the model on a large scale network to quantify the effectiveness of the proposed model.

A. IEEE 24 BUS RTS SYSTEM

In this section, the proposed model benefits are demonstrated by comparing them to the classical economic dispatch approach. The maximum renewable energy penetration, the total operating cost, and the power flow achieved for the proposed and classical economic dispatch model are used for comparison. The sizes of the two PV plants are 75 MW and 140 MW and the sizes of the two wind farms are 300 MW and 500 MW respectively. A total installed capacity of RES generators is 1015 MW. The IPP cost of energy for PV is 35 \$/MWh and 39 \$/MWh, while the cost of energy for wind is 34 \$/MWh and 30 \$/MWh respectively. Fig. 2, shows the forecasted RES generation.

The intermittent and variable RES information for the PV and wind power generators is given in Table 1 and Table 2 respectively, and the details of the transmission line data can be found in [13].

The details of the 32 thermal generator coefficients, capacity and ramp rates are provided in Table 3. There are 32 thermal generators which are connected to different buses on the IEEE 24 RTS network as shown in [49]. The details of the hourly demand requirements are shown in Table 4.

TABLE 1. PV solar irradiance profile for site 1 and 2.

Description	PV 1	PV 2
$K_c\ (W/m^2)$	150	150
$\Omega\ (W/m^2)$	1000	1000
β	0.5	0.600
κ_1	0.8	1.2
κ_2	4.13	5.4
$\sigma_1\ (W/m^2)$	150	140
$\sigma_2\ (W/m^2)$	900	980

TABLE 2. Wind speed profile for site 1 and 2.

Description	Wind 1	Wind 2
κ	1.70	2.0
$\sigma\ (m/s)$	6.653	5.0

TABLE 3. Thermal generator parameters.

Unit	No.	Pmin	Pmax	a_g	b_g	c_g	RU	DR
G1	5	2.40	12	0.025	25.5	24.4	48	60
G2	4	4.00	20	0.012	37.6	117.8	31	70
G3	6	0.00	50	0	0.5	0	60	60
G4	4	15.20	76	0.009	13.3	81.1	39	80
G5	3	25.00	100	0.006	18	217.9	51	74
G6	4	54.24	155	0.005	10.7	142.7	55	78
G7	3	68.95	197	0.003	23	259.1	55	99
G8	1	140.00	350	0.002	10.9	177.1	70	120
G9	2	100.00	400	0.002	7.5	311.9	51	100

TABLE 4. Forecasted demand.

Hour	Load (MW)	Hour	Load (MW)	Hour	Load (MW)
1	1495.2	9	2369.8	17	2460.3
2	1557.8	10	2480.3	18	2474.7
3	1532.7	11	2561.4	19	2461.0
4	1546.1	12	2419.8	20	2591.1
5	1620.6	13	2435.0	21	2624.7
6	1737.1	14	2371.3	22	2546.4
7	1872.2	15	2508.0	23	2309.4
8	2246.3	16	2662.7	24	1924.5

1) COMPARISON OF TRADITIONAL DED AND PROPOSED DED WITH RES OBLIGATION

In order to compare the traditional DED with the proposed model, it is important to make a distinction between the traditional model and the proposed model in Section II. For the traditional model, the Sigmoid function in (8), which represents the RO requirement, is ignored. Moreover, the traditional DED model is a single objective function optimisation problem. This means that the maximisation objective function is also ignored. Therefore, the only function involved in the traditional DED problem is the cost function for the thermal generators, the spinning reserve and the cost paid to IPPs for PV and wind power generation. The traditional DED is solved maintaining the spinning reserves as the maximum capacity of the largest generator. For the proposed model, we solve the DED with two conflicting objective functions; one which aims to minimise the total operating cost and the other which

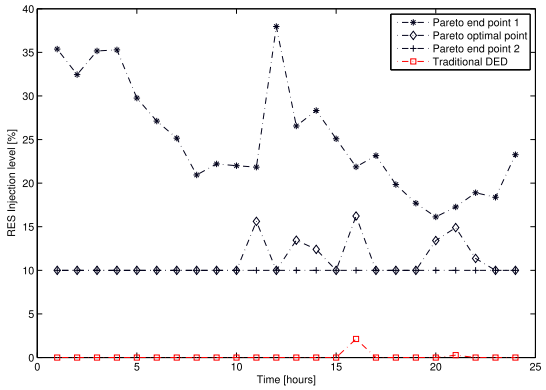

FIGURE 3. Hourly RES injection level between traditional DED and proposed model.

TABLE 5. Comparision between Pareto optimal solution and traditional DED.

Description	Pareto point	Traditional DED
Thermal (MWh)	45992.61	51820.18
PV (MWh)	1441.55	56.51000222
Wind (MWh)	4449.65	7.110003076
SR (MWh)	15565.14	15565.14
RES inj (%)	11.14%	0.12%
Cost ($)	1166356	1077753.11
Penalty cost ($)	-	1177753.11

TABLE 6. Impact of RES penetration on energy cost changes.

Description	100% cost	50% cost	10% cost
Thermal (MWh)	51820.18	50064.19	41066.34
PV (MWh)	56.51	1098.67	1292.03
Wind (MWh)	7.11	720.94	9525.44
SR (MWh)	15565.14	15565.14	15565.14
RES inj (%)	0.12%	3.51%	20.85%
Cost ($)	1077753.11	1 039 575.94	944 719.63
Penalty cost ($)	1177753.11	1 139 575.94	-

maximises the RES penetration level. A comparison of the RES penetration level between the classical DED and proposed model is shown in Fig. 3.

From Fig. 3, the RES penetration level for the traditional DED is lower than the Pareto optimal point, which means that the achieved RES penetration for the traditional DED is less than the required 10% obligation. As a result, a penalty is imposed on the traditional DED which results in a higher operating cost in comparison to the Pareto end point 2 as shown in Table 5. The impact of RES obligation is shown by the second anchor point which shows a consistent 10% RES obligation. A comparison of the thermal and RES generation is made in Table 5 which shows the 0.98% increase in operating cost between the Pareto optimal solution and the traditional DED.

The traditional DED RES penetration level is affected by the RES generation cost. Table 6, shows the changes in RES energy cost from 100%, 50% to 10%.

It is important to note that the maximum RES injected is achieved when the energy cost is reduced by 90%,

TABLE 7. Pareto anchor points.

Description	Objective: J_1 [$]	Objective: J_2 [MWh]
Minimisation point J^0	1,151,590	5188.4
Maximisation point J^{max}	1,587,000	12,463

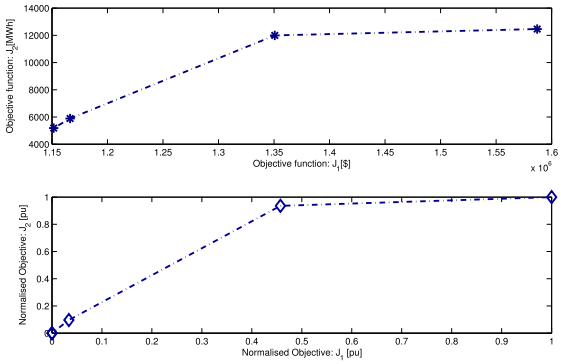

FIGURE 4. Normalised Pareto optimal solution for the IEEE 24 RTS system.

which results in 20.85% of RES penetration. The maximum RES achieved for the Pareto solution shown in Fig. 3, is 25% for the first end point which is 4% more than the traditional DED even with the reduction in RES energy cost. This demonstrates the effectiveness of the proposed model compared to the traditional DED.

2) PARETO FRONTIER SOLUTION

In order to find the Pareto frontier for the two objective functions presented in Section II, the first step is to find the minimisation and maximisation point of the two functions in order to normalise the overall function. These two points are called the Pareto anchor points. Table 7 presents the anchor points of the two objective functions.

The anchor points are evaluated by finding the letting λ_1 and λ_2 to be 0 and 1, which will provide the first anchor point for J_2 and when λ_1 and λ_2 are 1 and 0, then the second anchor point of J_1 provided as shown in Table 7. The Pareto frontiers are presented for the non-normalised and normalised Pareto solution in Fig. 4.

The Pareto optimal point shown in Fig. 4, corresponds to the total operating cost of $\$1,166,356$ and RES energy of 5891.2 MW. The Pareto solution is any solution that lies on the Pareto front curve, the anchor or end points correspond to the scenario where maximum RES penetration is achieved at a maximum operating cost or where a minimal operating cost is achieved with low to minimum RES penetration. A compromise solution is any solution that is on the Pareto front curve where enough RES penetration is achieved at an optimal operating cost with adequate spinning reserves. The RES penetration level for the first anchor point, Pareto point and last anchor point are shown in Fig. 5.

From the three Pareto points shown in Fig. 5, all the points satisfy the RES obligation requirement of 10%. In the first end point, a maximum of 38% of RES injection is achieved at 12h00 which corresponds to the maximum solar

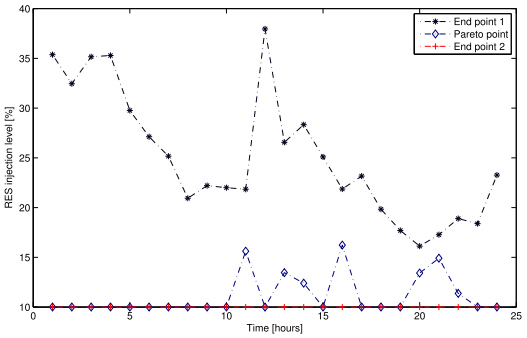

FIGURE 5. Pareto optimal solution for RES injection level of the anchor points and optimal point.

TABLE 8. Pareto optimal solution generation.

Description	End point 1	Optimal point	End point 2
Thermal Gen (MWh)	39420.85	45992.61	46695.42
PV Gen (MWh)	1479.71	1441.55	1441.55
Wind Gen (MWh)	10983.24	4449.65	3746.83
SR (MWh)	16295.7	15565.14	15565.14
PV Curtailment (MWh)	0	38.16	38.16
Wind Curtailment (MWh)	67.87	6601.47	7304.28

irradiance available. The overall average RES penetration achieved for the first anchor point is 25.07%. The optimal Pareto point chosen corresponds to the average RES injection level of 11.14% and in the last anchor point the achieved RES penetration level is 10%. It is important to note that the Pareto optimal solution shows the compromise between minimising the total operating cost while maximising the RES penetration and hence the RES penetration level has decreased in comparison to the first anchor point. In the last anchor point, the effectiveness of the proposed model is demonstrated by the achieved RES obligation of 10% with minimal operating cost.

A comparison of the total energy generated over a 24-hour period for the thermal generators, RES generators and required spinning reserves is shown in Table 8. In all the Pareto points, the thermal generator contributes the most energy as expected. In the first anchor point, more RES is generated and there is a small wind curtailment of 67.87 MWh and no PV curtailment. The average spinning reserve required is 31.41%. For one of the Pareto optimal points, the PV and wind curtailment is 38.16 MWh and 6601.47 MWh with the achieved RES injection level of 11.14%. The average spinning reserve required to guarantee continuity of power is 30% as shown in Table 8. For the last anchor point, the average RES injection level achieved is 10%, which complies with the RES obligation requirement. The curtailment of RES and minimum spinning reserves is also presented. The Pareto optimal frontier demonstrates the effectiveness of the proposed model by achieving the RES obligation and minimising the total operating costs.

3) IMPACT OF RO ON THE MODEL OPERATING COST

In this simulation study, the RO is varied from 5% to 50% at a step of 5%. The objective is to find the total RES penetration that can be achieved before any penalty can be imposed. The Pareto frontiers for each RES obligation are shown in Fig. 6.

The impact of RES obligation is variable. The RES obligation is achieved for the 5% to 20% case and any RES obligation over 25% to 50% is not achieved. The limitation in this case is based on the available forecasted generation, which means that if more RES generators are added to the network, the limit will increase in the same proportion. From Fig. 6, the Pareto frontier for 25% is the same as the Utopia line which means that anything over 25% will result in a dominant solution. The maximum RES penetration level is also indicated by the 20% RES Pareto front solution which forms the top limit for all the other Pareto curves. Therefore, from the normalised Pareto optimal solutions we observed that the Utopia line corresponds to a 25% RES penetration level. This also shows that any RES penetration over 25% is not attainable from the forecasted RES generation.

As expected, the total operating cost increases with the increase in RES obligation requirement due to the high RES energy cost. Table 9 shows the Pareto optimal point for the operating cost and the achieved RES penetration level for thermal and RES generators.

When the RES obligation changes, generally the spinning reserve changes in the same proportion. The reason for such a change is the spinning reserve requirement imposed by constraint (19), which requires that the thermal generators must be able to sustain the total demand without RES generation. It should also be noted that the total operating cost increases as the RES penetration increases and the transmission thermal limits are respected in all scenarios.

B. IEEE 118 BUS SYSTEM

The IEEE 118 bus system consists of 118 buses, 186 transmission lines, 91 load sides, 54 thermal generators, 10 RES generators with 5 PV and 5 wind farms. The total demand over a period of 24 hours is 126,854 MWh. In this case study, a RES obligation is maintained at 10% in order to investigate the impact of adding RES generators to the network. Moreover, an optimal RES obligation is investigated to attain the optimal cost of operating an energy mix that consists of thermal generators and RES generators. The ten RES generators are made of 5 PV plants and 5 wind farms with the following sizes: 500 MW, 200 MW, 150 MW, 140 MW and 260 MW for the wind farms; whilst the PV farms are made up of 75 MW, 140 MW, 300 MW, 28 MW and 66 MW. The total installed capacity of the RES generator is 1859 MW. A penalty of $100,000 is imposed if the RES obligation is not achieved. Table 10 and 11 show the site parameters for PV and wind plants respectively.

Fig. 7, shows the forecasted curves for demand and RES generation for the IEEE 118 bus system.

It is important to note that during winter seasons in South Africa wind speed can reach rated speed during the day in coastal areas which makes the forecasted wind power depicted in Fig. 7 possible [46].

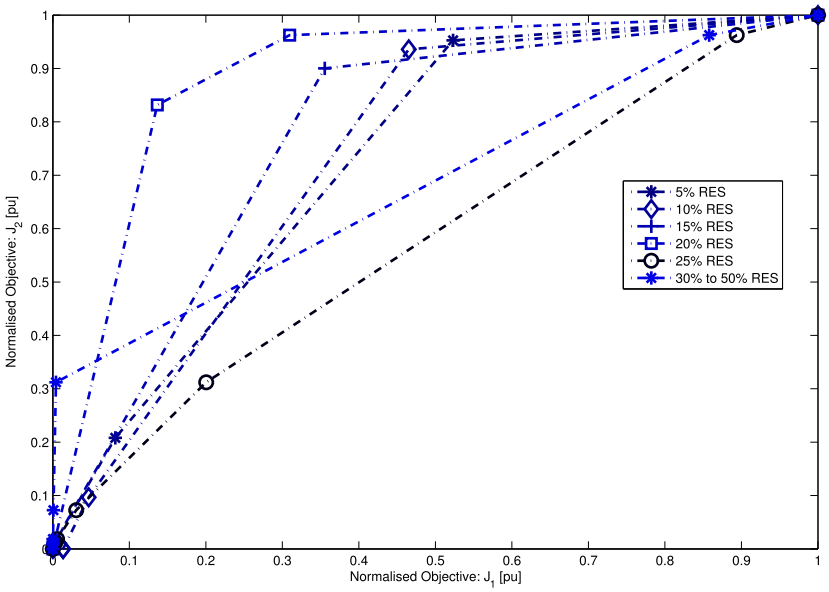

FIGURE 6. Pareto optimal solution for variation in RES penetration from 5% to 50%.

TABLE 9. Pareto optimal solution for a variable RES penetration level.

Description	5%	10%	15%	20%	25%
Thermal [MWh]	49290	45993	44101	39888	39888
PV[MWh]	1215	1292	1292	1480	1480
Wind[MWh]	1379	3896	6491	10517	10517
SR[MWh]	15565	15565	15565	15565	15565
Cost[$]	84968	40998	40998	15257	15257

TABLE 10. PV solar irradiance profile for site 1 to 5.

Description	PV 1	PV 2	PV 3	PV 4	PV5
$K_c\ (W/m^2)$	150	150	140	160	160
$\Omega\ (W/m^2)$	1000	1000	950	1100	1050
β	0.5	0.6	0.5	0.5	0.5
κ_1	0.8	1.2	0.8	1.6	0.9
κ_2	4.13	5.4	4.13	5.8	4.5
$\sigma_1\ (W/m^2)$	150	140	150	140	160
$\sigma_2\ (W/m^2)$	900	980	930	970	900

TABLE 11. Wind speed profile for site 1 to 5.

Description	Wind 1	Wind 2	Wind 3	Wind 4	Wind 5
κ	1.70	2.0	1.90	2.8	2.5
$\sigma\ (m/s)$	6.7	5.0	7.2	5.4	7

1) PARETO FRONTIER SOLUTION

The RES obligation is maintained at 10% and the energy cost for wind and PV plants is given in Annexure A, Table 14. As part of the Pareto solution, Table 12 shows the anchor points and one of the points on the Pareto frontier curve.

The Pareto point in Table 12, shows the trade-off between achieving maximum RES penetration at a high operating cost or a scenario of low-RES penetration at a minimum

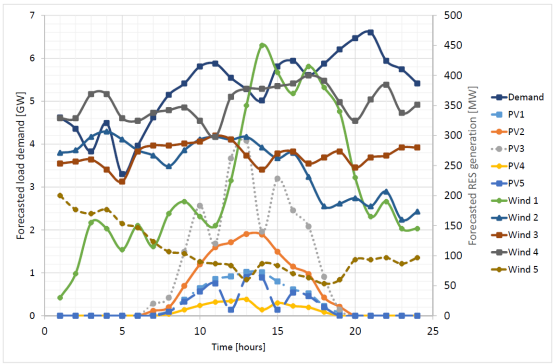

FIGURE 7. Forecasted demand and RES generation for IEEE 118 bus system.

TABLE 12. Pareto anchor points.

Description	Objective: J_1 [$]	Objective: J_2 [MWh]
Minimisation point J^0	3,038,231	13,043
Pareto point	3,041,191	13,087
Maximisation point J^{max}	4,703,000	32,115

operating cost. Therefore, any solution on the Pareto front will realise a non-dominant solution. Fig. 8, shows the Pareto frontier curves for non-normalised and normalised.

In Fig. 8, the minimum point corresponds to the RES obligation requirement of 10% which demonstrates the effectiveness of the proposed model. A 10% RES obligation is achieved, and the total operating cost is $3,038,231. The RES penetration levels for the two end points and one of the Pareto points are shown in Fig 9.

From Fig. 9, the average RES penetration level for the first anchor point is 25.46% and the minimum average RES

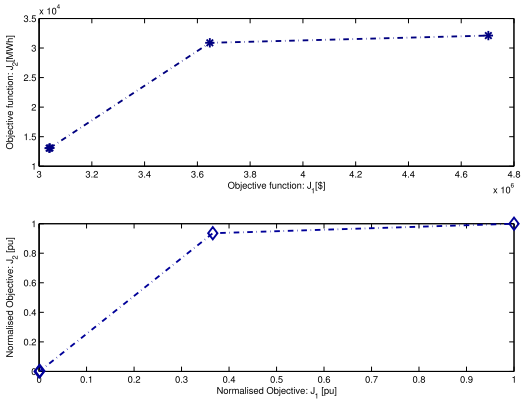

FIGURE 8. Pareto frontier solution for IEEE 118 bus system.

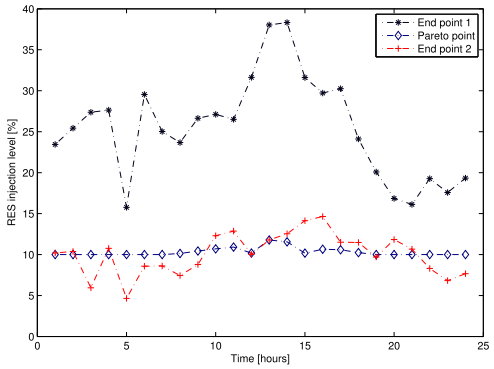

FIGURE 9. Pareto optimal solution for RES injection level of the anchor points and optimal point.

TABLE 13. Pareto optimal solution generation.

Description	End point 1	Pareto point	End point 2
Thermal Gen (MWh)	95096	114125	114169
PV Gen (MWh)	3788	1324	1324
Wind Gen (MWh)	28327	11762	11719
SR (MWh)	38934	38056	38056
PV Curtailment (MWh)	0	2464	2464
Wind Curtailment (MWh)	435.3	17000	17044
RES injection (%)	25.46	10.31	10.07

penetration corresponds to the last anchor point which is 10.07%. In addition to the anchor points shown in Fig. 9, a single point in the Pareto frontier curve depicted shows an average RES penetration level of 10.31%; this means the RES obligation is attained for this scenario. Table 13 shows the achieved generation for thermal and RES generators, the minimum spinning reserves required, the curtailment of RES generators and the achieved RES penetration for each Pareto point.

The RES penetration achieved on the first anchor point demonstrates the typical Pareto solution compromise, which means that for a maximum RES penetration level, the total operating cost is also high. On the contrary, for the first end point, where more RES generation is injected, there is no curtailment for PV generators and a small curtailment for wind generators. This curtailment corresponds to

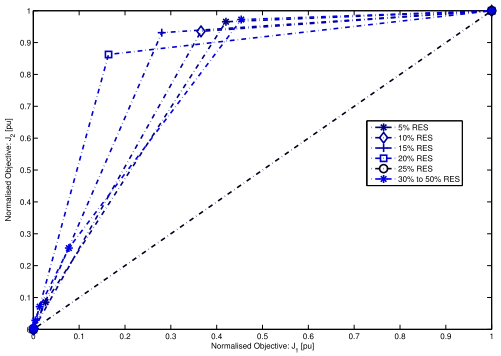

FIGURE 10. Pareto optimal solution for variation in RES penetration from 5% to 50%.

transmission line limit. A significant curtailment is shown for the other Pareto points, however, in all Pareto curves the RES obligation is still attained. This demonstrates the effectiveness of the proposed model which means that a solution that rests anywhere on the Pareto frontier will realise an optimal solution with a compromise between operating cost and RES penetration level.

2) IMPACT OF RO ON THE MODEL OPERATING COST

In this scenario, the impact of varying RES penetration level is investigated to ascertain the maximum RES penetration that can be attained for the forecasted RES generation. As mentioned in the previous case study, the RES penetration level is varied from 5% to 50% at a step of 5%. It is important to note that the task of selecting an adequate solution from a set of optimal solutions is difficult, therefore, to overcome this challenge a sequence of Pareto optimal solutions is presented in Fig. 10 for different RES penetration levels.

The different Pareto front optimal solutions presented in Fig. 10, show the impact of RES penetration level. Firstly, we observed that the maximum RES penetration achieved for the IEEE 118 bus system corresponds to the 25% RES penetration Pareto frontier. This means any Pareto optimal solution that is less than 25% RES penetration is attainable without the need for penalty. The 25% penetration level is the Utopia line for the bi-optimisation problem. It was also observed that the 20% RES penetration level is the top Pareto optimal solution that covers all the other Pareto solutions, which means an optimal Pareto solution for the forecasted RES generation lies in the range of 20% to 25% and any solution over 25% of RES penetration is unattainable due to the limitation in the forecasted RES generation.

V. DISCUSSION

In Section IV, we presented a case study that investigated the impact of RES penetration from a RO point of view. Three case were presented; in the first case a comparative study between the classical SCED and the proposed RO is investigated. Then the impact of varying the RES energy cost is investigated and compared to the RO model to better appreciate the proposed model robustness to attain the RO.

In the second case study a Pareto optimal solution is presented which shows a compromise between maximising the RES energy penetration and minimising the total operating cost while maintaining the renewable energy quota. The final case study shows the impact of varying the RES obligation on the sensitivity of the model. We vary the obligation target from 5% to 50% with a step of 5% to show its impact on the total operating cost and the RES penetration level.

The impact of increasing RES penetration level using RO policy framework it is better appreciated when we compared the classical SCED. Fig. 3 shows a comparison between classical SCED and the RO SCED model. The RO model shows a Pareto optimal solution for the end points and optimal point, i.e., minimum, optimal and maximum Pareto point. The RO model can meet the required renewable energy quota compared to the classical SCED model. The classical model shows poor performance in terms of RES penetration and this is due to the cost associated with procuring RES energy which is higher than the traditional thermal generator energy cost. It is interesting to note that for the RO model, the cost of RES is not an important factor in achieving the RES penetration. This is due to the penalty imposed for not achieving RES which is much higher compared to the RES energy cost, and hence in all cases the RO is achieved. To overcome the impact of RES energy cost, Table 6 shows the RES penetration level for different energy cost reduction, i.e., from nominal to 90% RES energy cost reduction. Note that in these simulation studies, the RO is set as 10%. It is clear from the simulation results that RES obligation is achieved only when the RES energy cost is reduced by 90%. The first case study demonstrates the importance of including a penalty cost in the RO model by ensuring that the renewable energy quota is achieved. Therefore, the RO models presented in Section II is dependent on the penalty cost which mean that if the penalty cost is low then the RES quota is ignored, and if it high then the RES obligation is achieved based on the available resource and the line thermal limits. This part of the model demonstrates a useful tool for policy makers to encourage energy mix. When we compare the total operating cost of the classical SCED and the proposed RO model we notice that the proposed model operating cost is lower than the classical SCED cost and this is due to the penalty cost imposed for not achieving the RO quota. However, when the RES energy cost is reduced by 90%, the classical SCED operating cost becomes competitive and the renewable energy quota is achieved. This means that for the RES to be competitive on the classical model, its energy cost must be lower than the thermal generators.

The Pareto optimal solution presented in Section IV shows that there is not a single solution to the model but several optimal solutions. This is clearly demonstrated by Figs. 6 and 10 for the IEEE 24 RTS and 118 bus system. This means that if the first objective function is set to zero, then the overall optimisation problem changes to a maximisation of RES energy penetration that can be achieved without any curtailment. The solution to this problem corresponds to the first end point of the Pareto frontier curve. On the contrary, if the second objective function is set to zero, then the aim simply turns into minimising the total operating while achieving the minimum RES quota set out by the SO and this point is also known as the Pareto end point. These two points are the anchors of the Pareto frontier curves and all the points that lie on the curve forms the Pareto frontier as demonstrated in Fig. 4 and 9. The impact of varying RO is illustrated by the Pareto frontiers shown in Fig. 6 and 10 for the two test systems. The variation in the Pareto frontier curves is due to different RO requirements. For example, if we consider Fig. 6 for IEEE 24 RTS system, we can observe that the RO is achieved from 5% all the way to 25% of RES penetration. The 25% Pareto frontier forms a Utopia line which shows the maximum RES that can be achieved without any penalty. A RES penetration level over 25% is shown in the same figure which is far less than the RES penetration of all Pareto frontier curves. This demonstrates the effectiveness of the proposed RO model to meet different RES quota obligation.

To summarise the finding of Section IV, a RO model leads to higher RES penetration while minimising the total operating cost and spinning reserves. The RO model shows that the only limiting factor to maximum RES penetration is the available resource and transmission thermal limit. Although the CO_2 emission reduction is not quantified in this study, we can infer that the RO model has a potential to decrease CO_2 emission and significantly reduce the operating cost of thermal generators.

VI. CONCLUSION

In this paper, a new DED model with RES obligation is presented which integrates RES generation to maximise the RES penetration while minimising the total operating cost and the spinning reserves. The approach presented determines the optimal RES penetration level that minimises the operating cost and spinning reserves while providing continuity of power supply. A bi-optimisation problem is presented that minimises the operating cost and maximises the RES energy penetration. The formulation shows a trade-off between maximum RES penetration and minimum operating costs. Generally, the proposed model has the advantage of achieving a maximum RES penetration based on the RES obligation and minimising the required spinning reserves and total operating costs. In all the case studies presented, the power transfer flow is respected. The results of the case studies demonstrate the robustness of the proposed optimisation model in terms of RES obligation requirement and optimal operating cost and a trade-off between economical operation and maximum RES penetration.

APPENDIX

DATA USED FOR THE MODIFIED IEEE 24 RELIABILITY TEST SYSTEM (RTS) AND IEEE 118 BUS SYSTEM

The spinning reserve costs for the 32 and 54 generator system are given in Table 14; all the costs are in $\$/MWh$.

The RES cost for IEEE 118 bus is shown in Table 15, all costs are in US dollars.

TABLE 14. IEEE 24 RTS and 118 bus system spinning reserve costs [50].

SR 1 - 11	SR 13 - 22	SR 23 - 33	SR 34 - 44	SR 45 - 55
30	12	40	20	22
28	60	45	40	27
25	18	27	37	19
20	0 & 20	35	18	33
40	30	12	22	50
45	22	45	32	33
55	55	45	45	33
12	35	33	34	54
10	12	20	10.5	35
20	12	12	15	14
40	18	40	18	0

TABLE 15. IEEE 118 bus system RES cost in $/*MWh* [51].

Wind($/MWh$)	PV ($/MWh$)
44	53
40	38
46	51
53	45
30	39

ACKNOWLEDGMENT

The authors gratefully acknowledge the contributions of M. Sibiya, N. S. Khumalo, N. Khumalo, and R. Gwandira for their work on the original version of this document. They were also grateful to the reviewers and editors for their valuable input.

REFERENCES

[1] EU. *Renewable Energy Directive 2009/28/EU*. Accessed: 2019. [Online]. Available: https://www.dccae.gov.ie/en-ie/energy/topics/Renewable-Energy

[2] Department of Energy. *Integrated Resource Plan*. Accessed: 2019. [Online]. Available: http://www.energy.gov.za/IRP

[3] G. Shrimali and E. Baker, "Optimal feed-in tariff schedules," *IEEE Trans. Eng. Manag.*, vol. 59, no. 2, pp. 310–322, May 2012.

[4] G. Wang, V. Kekatos, A. J. Conejo, and G. B. Giannakis, "Ergodic energy management leveraging resource variability in distribution grids," *IEEE Trans. Power Syst.*, vol. 31, no. 6, pp. 4765–4775, Nov. 2016.

[5] Y. Zhou, L. Wang, and J. D. McCalley, "Designing effective and efficient incentive policies for renewable energy in generation expansion planning," *Appl. Energy*, vol. 88, no. 6, pp. 2201–2209, Jun. 2011.

[6] F. Careri, C. Genesi, P. Marannino, M. Montagna, S. Rossi, and I. Siviero, "Generation expansion planning in the age of green economy," *IEEE Trans. Power Syst.*, vol. 26, no. 4, pp. 2214–2223, Nov. 2011.

[7] J. P. Chaves-Avila, F. Banez-Chicharro, and A. Ramos, "Impact of support schemes and market rules on renewable electricity generation and system operation: The Spanish case," *IET Renew. Power Gener.*, vol. 11, no. 3, pp. 238–244, Feb. 2017.

[8] K. Geetha, V. Sharmila Deve, and K. Keerthivasan, "Design of economic dispatch model for Gencos with thermal and wind powered generators," *Int. J. Electr. Power Energy Syst.*, vol. 68, pp. 222–232, Jun. 2015.

[9] L. Deng, B. F. Hobbs, and P. Renson, "What is the cost of negative bidding by wind? A unit commitment analysis of cost and emissions," *IEEE Trans. Power Syst.*, vol. 30, no. 4, pp. 1805–1814, Jul. 2015.

[10] D. W. Ross and S. Kim, "Dynamic economic dispatch of generation," *IEEE Trans. Power App. Syst.*, vol. PAS-99, no. 6, pp. 2060–2068, Nov. 1980.

[11] T. Bechert and H. Kwatny, "On the optimal dynamic dispatch of real power," *IEEE Trans. Power App. Syst.*, vol. PAS-91, no. 3, pp. 889–898, May 1972.

[12] M. Hedayati-Mehdiabadi, P. Balasubramanian, K. W. Hedman, and J. Zhang, "Market implications of wind reserve margin," *IEEE Trans. Power Syst.*, vol. 33, no. 5, pp. 5161–5170, Sep. 2018.

[13] G. Liu and K. Tomsovic, "Quantifying spinning reserve in systems with significant wind power penetration," *IEEE Trans. Power Syst.*, vol. 27, no. 4, pp. 2385–2393, Nov. 2012.

[14] L. Yao, X. Wang, C. Duan, J. Guo, X. Wu, and Y. Zhang, "Data-driven distributionally robust reserve and energy scheduling over Wasserstein balls," *IET Gener., Transmiss. Distrib.*, vol. 12, no. 1, pp. 178–189, Jan. 2018.

[15] T. Adefarati and R. C. Bansal, "Integration of renewable distributed generators into the distribution system: A review," *IET Renew. Power Gener.*, vol. 10, no. 7, pp. 873–884, Aug. 2016.

[16] Y. Ma, Y. Hao, S. Zhao, and H. Bi, "Security constrained economic dispatch of wind-integrated power system considering optimal system state selection," *IET Gener., Transmiss. Distrib.*, vol. 11, no. 1, pp. 27–36, Jan. 2017.

[17] V. Hinojosa and F. Gonzalez-Longatt, "Preventive security-constrained DCOPF formulation using power transmission distribution factors and line outage distribution factors," *Energies*, vol. 11, no. 6, pp. 1497–1510, Jun. 2018.

[18] Z. Song, L. Goel, and P. Wang, "Optimal spinning reserve allocation in deregulated power systems," *IEE Proc. Gener., Transmiss. Distrib.*, vol. 152, no. 4, pp. 483–488, Jul. 2005.

[19] T. Qiu, B. Xu, Y. Wang, Y. Dvorkin, and D. S. Kirschen, "Stochastic multistage coplanning of transmission expansion and energy storage," *IEEE Trans. Power Syst.*, vol. 32, no. 1, pp. 643–651, Jan. 2017.

[20] H. Daneshi and A. K. Srivastava, "Security-constrained unit commitment with wind generation and compressed air energy storage," *IET Gener., Transmiss. Distrib.*, vol. 6, no. 2, pp. 167–175, 2012.

[21] Y. Fu, M. Liu, and L. Li, "Multiobjective stochastic economic dispatch with variable wind generation using scenario-based decomposition and asynchronous block iteration," *IEEE Trans. Sustain. Energy*, vol. 7, no. 1, pp. 139–149, Jan. 2016.

[22] S. S. Reddy, B. K. Panigrahi, R. Kundu, R. Mukherjee, and S. Debchoudhury, "Energy and spinning reserve scheduling for a wind-thermal power system using CMA-ES with mean learning technique," *Int. J. Electr. Power Energy Syst.*, vol. 53, pp. 113–122, Dec. 2013.

[23] J. Hetzer, D. C. Yu, and K. Bhattarai, "An economic dispatch model incorporating wind power," *IEEE Trans. Energy Convers.*, vol. 23, no. 2, pp. 603–611, Jun. 2008.

[24] S. S. Reddy, P. R. Bijwe, and A. R. Abhyankar, "Real-time economic dispatch considering renewable power generation variability and uncertainty over scheduling period," *IEEE Syst. J.*, vol. 9, no. 4, pp. 1440–1451, Dec. 2015.

[25] DBEI. *Renewable Obligation 2019/20*. Accessed: 2019. [Online]. Available: https://assets.publishing.service.gov.uk/

[26] DBEI. *Renewable Obligation Guidelines*. Accessed: 2019. [Online]. Available: https://www.gov.uk/guidance/calculatingrec

[27] L. Mokgonyana, J. Zhang, H. Li, and Y. Hu, "Optimal location and capacity planning for distributed generation with independent power production and self-generation," *Appl. Energy*, vol. 188, pp. 140–150, Feb. 2017.

[28] G. Gurkan and R. Langestraat, "Modeling and analysis of renewable energy obligations and technology banding in the UK electricty market," *Energy Policy*, vol. 70, pp. 85–95, Apr. 2014.

[29] H. Zhou, "Impacts of renewables obligation with recycling of the buy-out fund," *Energy Policy*, vol. 46, pp. 284–291, Jul. 2012.

[30] G. Wood and S. Dow, "What lessons have been learned in reforming the renewables obligation? An analysis of internal and external failures in UK renewable energy policy," *Energy Policy*, vol. 39, no. 5, pp. 2228–2244, May 2011.

[31] X. Li, L. Fang, Z. Lu, J. Zhang, and H. Zhao, "A line flow granular computing approach for economic dispatch with line constraints," *IEEE Trans. Power Syst.*, vol. 32, no. 6, pp. 4832–4842, Nov. 2017.

[32] B. Stott, J. Jardim, and O. Alsac, "DC power flow revisited," *IEEE Trans. Power Syst.*, vol. 24, no. 3, pp. 1290–1300, Aug. 2009.

[33] C. Roman and W. Rosehart, "Evenly distributed Pareto points in multi-objective optimal power flow," *IEEE Trans. Power Syst.*, vol. 21, no. 2, pp. 1011–1012, May 2006.

[34] J. S. Arora, *Introduction to Optimum Design*, 4th ed. Amsterdam, The Netherlands: Elsevier, 2017.

[35] K. Y. Lee and M. A. El-Sharkawi, Eds., *Modern Heuristic Optimization Techniques: Theory and Applications to Power Systems*, vol. 39. Hoboken, NJ, USA: Wiley, 2018.

[36] R. C. Bansal, Ed., *Handbook of Distributed Generation: Electric Power Technologies, Economics and Environmental Impacts*. Cham, Switzerland: Springer, 2017.

[37] M. R. Patel, *Wind and Solar Power Systems Design, Analysis and Operation*, 2nd ed. New York, NY, USA: Taylor & Fracis, 2006.
[38] J. F. Manwell, J. G. McGowan, and A. L. Rogers, *Wind Energy Explained: Theory, Design and Application*, 2nd ed. Hoboken, NJ, USA: Wiley, 2009.
[39] X. Liu and W. Xu, "Minimum emission dispatch constrained by stochastic wind power availability and cost," *IEEE Trans. Power Syst.*, vol. 25, no. 3, pp. 1705–1713, Aug. 2010.
[40] P. Meibom, R. Barth, B. Hasche, H. Brand, C. Weber, and M. O'Malley, "Stochastic optimization model to study the operational impacts of high wind penetrations in Ireland," *IEEE Trans. Power Syst.*, vol. 26, no. 3, pp. 1367–1379, Aug. 2011.
[41] R.-H. Liang and J.-H. Liao, "A fuzzy-optimization approach for generation scheduling with wind and solar energy systems," *IEEE Trans. Power Syst.*, vol. 22, no. 4, pp. 1665–1674, Nov. 2007.
[42] C. Lupangu and R. C. Bansal, "A review of technical issues on the development of photovoltaic systems," *Renew. Sustain. Energy Rev.*, vol. 73, no. 6, pp. 950–965, Jun. 2017.
[43] K. Nghitevelekwa and R. C. Bansal, "A review of generation dispatch with large-scale Photovoltaic (PV) systems," *Renew. Sustain. Energy Rev.*, vol. 81, pp. 615–624, Jan. 2018.
[44] H. Kanchev, F. Colas, V. Lazarov, and B. Francois, "Emission reduction and economical optimization of an urban microgrid operation including dispatched PV-based active generators," *IEEE Trans. Sustain. Energy*, vol. 5, no. 4, pp. 1397–1405, Oct. 2014.
[45] M. Zhang, X. Ai, J. Fang, W. Yao, W. Zuo, Z. Chen, and J. Wen, "A systematic approach for the joint dispatch of energy and reserve incorporating demand response," *Appl. Energy*, vol. 230, pp. 1279–1291, Nov. 2018.
[46] WASA. *Wind Atlas for South African Projects*. Accessed: 2019. [Online]. Available: http://wasa.csir.co.za/web/welcome.aspx
[47] SODA. *Solar Radiation Data*. Accessed: 2019. [Online]. Available: http://www.soda-pro.com/home
[48] R. D. Zimmerman, and C. E. Murillo-Sanchez. *MATPOWER*. Accessed: 2019. [Online]. Available: https://matpower.org
[49] G. Liu, "Generation scheduling for power systems with demand response and high penetration of wind energy," Ph.D. dissertation, Univ. Tennessee, Knoxville, TN, USA, 2014.
[50] A. G. Tsikalakis and N. D. Hatziargyriou, "Centralized control for optimizing microgrids operation," *IEEE Trans. Energy Convers.*, vol. 23, no. 1, pp. 241–248, Mar. 2008.
[51] Eskom. *Eskom Financial Statement*. Accessed: 2019. [Online]. Available: http://www.eskom.co.za/IR2018/Documents/Eskom2018AFS

THABO G. HLALELE received the B.Eng. and M.Eng. degrees in electrical engineering from the University of Pretoria, South Africa, where he is currently pursuing the Ph.D. degree in electrical engineering. His research interest includes power system optimization, protection, control, and integrating renewable energy sources. He is also a Professional Engineer registered with the Engineering Council of South Africa and a member of SAIEE.

RAJ M. NAIDOO (Senior Member, IEEE) received the Ph.D. degree in engineering from the University of Cape Town. He is currently an Associate Professor of power engineering with the University of Pretoria and the Director of smart grid research. He has extensive experience in power and energy systems. His expertise ranges from power and energy systems to product development in the area where the power grid meets IoT. He co-founded Enermatics Energy (Pty) Ltd., in 2007. This was subsequently sold to a listed company. He then co-founded eWyze (Pty) Ltd., an electrical and energy management company, where he is also the Director. He has consulted to a number of blue chip companies and worked for Eskom in the fields of power quality and network planning. He has supervised a number of master's and Ph.D. students in the field. He has published articles in leading conferences and journals.

JIANGFENG ZHANG received the Ph.D. degree in mathematics and the second Ph.D. degree in electrical engineering. He is currently an Associate Professor with the Department of Automotive Engineering, Clemson University at Greenville, USA. His research interests include electric vehicles, smart grids, and renewable energy. He is also a Fellow of IET, a Chartered Engineer, and a member of the IFAC TC6.3 (Power and Energy Systems). He is an Associate Editor of *IET Renewable Power Generation* and *IET Smart Grid*.

RAMESH C. BANSAL (Senior Member, IEEE) was a Professor and the Group Head (power) with the ECE Department, University of Pretoria (UP), South Africa. Prior to his appointment at UP, he was employed by The University of Queensland, Australia, The University of the South Pacific, Fiji, BITS Pilani, India, and Civil Construction Wing, All India Radio. He is currently a Professor with the Department of Electrical Engineering, University of Sharjah. He has significant experience of collaborating with industry and Government Organizations. He has made significant contribution to the development and delivery of B.S. and M.E. programmes for utilities. He has extensive experience in the design and delivery of CPD programmes for professional engineers. He has more than 25 years of diversified experience of research, scholarship of teaching and learning, accreditation, industrial, and academic leadership in several countries. He has carried out research and consultancy and attracted significant funding from Industry and Government Organisations. He has published over 300 journal articles, presented papers at conferences, and books and chapters in books. He has Google citations of over 8500 and H-index of 41. He has supervised 20 Ph.D. students, four Postdoctoral Researchers, and currently supervising five Ph.D. students. His diversified research interests are in the areas of renewable energy (wind, PV, DG, micro grid), and smart grid.

Prof. Bansal is a Fellow and Chartered Engineer of IET, U.K., and a Fellow the Institution of Engineers, Australia, the Institution of Engineers, India, and SAIEE. He is an Editor of several highly regarded journals, IET-RPG, and the IEEE Systems Journal.